Anisotropic Photodetachment of Positronium Negative Ions with Linearly Polarized Light

Koji Michishio,[1,2,*] Luca Chiari,[3,2] Fumi Tanaka,[2] and Yasuyuki Nagashima[2]
[1]National Institute of Advanced Industrial Science and Technology (AIST), 1-1-1 Umezono, Tsukuba, Ibaraki 305-8568, Japan
[2]Department of Physics, Tokyo University of Science, 1-3 Kagurazaka, Shinjuku, Tokyo 162-8601, Japan
[3]Department of Applied Chemistry and Biotechnology, Faculty of Engineering, Chiba University, 1-33 Yayoi, Inage, Chiba 263-8522, Japan

(Received 14 January 2024; revised 25 March 2024; accepted 18 April 2024; published 14 May 2024)

We report on the anisotropic photodetachment of positronium negative ions, followed by the dissociation into p-wave electrons and positronium atoms, with a linearly polarized laser beam. We have observed a strong recoil effect of the photoelectrons on the translation momentum of the dissociated positronium atoms. With polarization angle-resolved measurements, the asymmetry parameter of the photoemission angular distribution of the ions at a photon energy of 1.165 eV was determined to be $1.97 \pm 0.04(\text{stat}) \pm 0.07(\text{syst})$, in agreement with a theoretical prediction. The present method can be applied to explore the unrevealed dissociation dynamics of exotic particle systems and their manipulation with polarized light.

DOI: 10.1103/PhysRevLett.132.203001

The photoionization and photodetachment of atoms, molecules, and ions are fundamental processes and provide valuable information on their electronic structures and dynamics [1]. Revealing the dynamics, precisely determining the momentum vectors of photofragments, is particularly important for identifying the kinetic energy release and quantum state, as well as the photoelectron angular distribution. A variety of spectrometric methods have been used to investigate these variables, including the Doppler-effect method [2,3], translation-energy spectroscopy [4], photofragment velocity map imaging [5–7] and coincidence momentum imaging techniques such as cold target recoil ion momentum spectroscopy [8] and related methods [9]. On the other hand, research exploring photo-induced dynamics from dissociated fragments has not been extended to exotic particle species, including particles and their antiparticles, e.g., positrons, muons, and antiprotons, etc. Such research would serve as a new testing ground for quantum chemical theories due to the unique mass ratios of the constituents. However, the rare and short-lived nature of those particles, as well as the lack of cold and point sources, have so far hindered their applicability to this kind of experiment.

Positronium (Ps) is a bound state of an electron and its antimatter counterpart, the positron. Ps has two spin eigenstates depending on the total spin, S, of the constituents; *para*-Ps ($S = 0$) atoms decay into two photons with a lifetime of 125 ps, while *ortho*-Ps ($S = 1$) atoms decay into three photons with a relatively long lifetime of 142 ns. Ps can also bind an electron to form a Ps negative ion (Ps^-, $^1S^e$) with a lifetime of 479 ps. Ps^- is one of the simplest three-body Coulomb systems, lying between the atomic limit (H^-) and molecular limit (H_2^+) due to the unique mass ratio of its constituents. Its electronic structure and dynamics have been of great interest and the subject of numerous quantum chemistry calculations [10]. Only recently, with the realization of an efficient Ps^- ion source with tungsten coated by submonolayer alkali-metals [11], spectroscopic studies of this exotic ion with tunable lasers have become feasible [12,13]. However, because of the extremely short lifetime and the source quality of Ps^- ions, the aforementioned studies exploring the photo-induced dissociation dynamics of this exotic ion have not been realized. Moreover, if the anisotropy of the dissociation can be controlled by polarized light, it may be possible to manipulate the motion and quality of the Ps beam formed by the photodetachment of Ps^- ions [14]. This technique can be used to generate tunable coherent Ps beams, which is an essential requirement in diffraction-based surface analysis [15] with electrically neutral Ps, Ps -atom and -molecule collisions [16] and in the verification of gravitational effects acting on Ps [17,18].

In this Letter, we present the experimental demonstration of the recoil momentum spectroscopy in the one-photon detachment of the Ps^- ions, leading to the dissociation of p-wave electrons and Ps atoms. Time-of-flight measurements of the dissociated Ps fragments result in the observation of strong photoelectron recoil to Ps atoms. The photodetachment of Ps^- ions, followed by fragmentation into particles with similar masses, exhibits similarities to the kinematics of molecular dissociations that undergo significant recoil between fragments and residual, impacting on the momentum of each other [19,20]. The anisotropy parameter

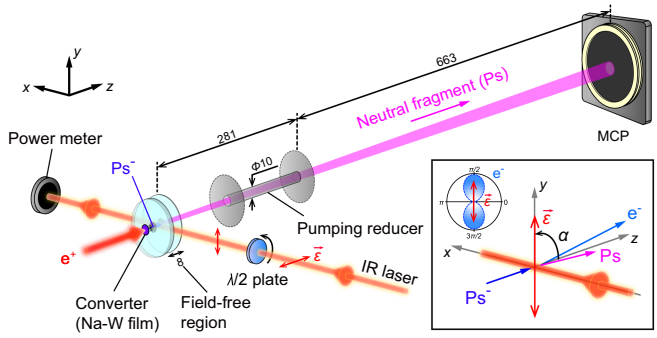

FIG. 1. Experimental setup for the recoil momentum spectroscopy of Ps^- ions. The inset shows the geometry of the Ps^- photodetachment in the laboratory frame, where the Ps^- ions traveling along the z-axis are photodetached by an IR laser beam propagating along the x axis. The distribution of the photoelectrons is parametrized by the polarization angle, α, between the traveling direction of the Ps^- ions and the polarization vector, $\vec{\varepsilon}$, rotated on the $y-z$ plane. The upper left figure in the inset shows the angular distribution of p-wave photoelectron emission from Ps^-. In the center of mass frame, the photoelectrons are emitted with respect to the polarization vector, giving a recoil momentum in the opposite direction to the fragment Ps atoms. The units of the distances indicated in the figure are mm.

that characterizes the photoemission angular distribution of the Ps^- ions is also determined by varying the polarization vector of the linearly polarized laser beam.

The experiment utilizes a high-quality Ps beam apparatus constructed at Tokyo University of Science. The apparatus details are described elsewhere [14]. Figure 1 exhibits the experimental setup for the recoil momentum spectroscopy of the Ps^- ions. Nanosecond positron bursts having a temporal width (FWHM) of 2 ns and a 50 Hz repetition from a positron trap [21] impinge onto an e^+-to-Ps^- converter made of a submonolayer Na-coated W film (100 nm thickness). A fraction of the positrons thermalized in the film diffuses to the opposite Na-coated surface, where they are converted to Ps^- ions efficiently [22]. The kinetic energy of Ps^- leaving the Na-coated W surface corresponds to its affinity value of $\delta E \sim 3.4$ eV [11]. To accelerate the ions along the z axis, a potential gap, $V_{\rm acc}$, is applied between the film and two grid electrodes located in front of the film. They are transported in the field-free region formed between the grids placed 8 mm apart and then are illuminated with an infrared (IR) laser beam ($\lambda = 1064$ nm) propagating along the x axis. The laser beam has a temporal width of 10 ns full width at half maximum (FWHM) and a nominal energy of 0.1 J/pulse. The laser source is a Q-switch Nd:YAG laser (Spectra-Physics, Quanta-Ray Pro-290) operated at a 50 Hz repetition. The output beam is linearly polarized with a polarization degree of 98%. To adjust the polarization vector angle, α, with respect to the Ps^- travel direction, an air-gap type $\lambda/2$ plate (SIGMAKOKI, WPQG-10640-2M) is placed on the optical axis. The $\alpha = 0$ angle is calibrated to within ± 1 degree by a linear polarizer mounted on the vacuum chamber.

Ps^- ions are dissociated into a photoelectron and a Ps atom by the laser illumination. The kinetic energy release, $E_{\rm KER} = hc/\lambda - E_{\rm B}$, is allocated to the photoelectron ($2E_{\rm KER}/3$) and Ps that undergoes recoil ($E_{\rm KER}/3$), where h and c are the Planck constant and speed of light, respectively, and $E_{\rm B}$ is the electron affinity of Ps. Since the charged particles from the converter are eliminated, as described in Appendix A, the electrically neutral Ps atoms (long-lived o-Ps only) travel along the z axis and are subsequently detected by a microchannel plate (MCP) with an effective diameter of 80 mm. The present photodetachment scheme yields an $E_{\rm KER}$ as low as 0.8 eV, which is 2 orders of magnitude smaller than the possible kinetic energy of the Ps atoms (several hundred eV). For this reason, we extended the drift length of the Ps atoms to $L = 944 \pm 1$ mm, roughly double the previous length [14], to magnify the recoil effect. The output signals of the detector are fed into a fast amplifier (ReontDek, FAMP), then acquired with a 1.25 GS/s-ADC module (RoentDek, FADC), and finally recorded as time-of-flight (TOF) spectra with the laser illumination as time zero. The TOF of Ps atoms is acquired as a function of α and $V_{\rm acc}$ in order to examine their response to the z-axis projection momentum. Note that a pumping reducer tube with a 10 mm inner diameter connects the converter region to the detector region, which ensures that the converter region remains in an ultrahigh vacuum condition of 1×10^{-8} Pa to sustain the converter efficiency [22].

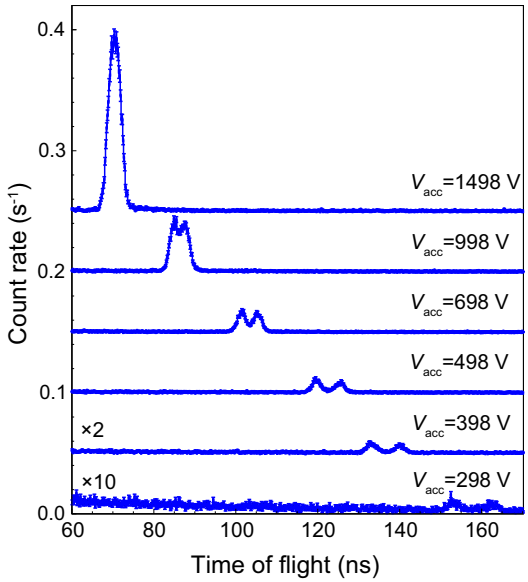

FIG. 2. Time-of-flight spectra of the fragment Ps atoms with different acceleration voltages of the Ps^- ions, $V_{\rm acc}$. The polarization angle was set to $\alpha = 0$ (π polarization). Each spectrum was accumulated over 4200 s.

However, this arrangement causes a distortion of the TOF spectra, as detailed later on.

Figure 2 exhibits the TOF spectra of Ps atoms as a function of V_{acc}, in the $\alpha = 0$ condition (π polarization). The mean TOF values are correspondingly delayed as V_{acc} decreases, which is consistent with that of Ps atoms formed by the photodetachment of the accelerated Ps^- ions. This namely indicates that the average velocity (kinetic energy) of the electrically neutral Ps can be controlled by V_{acc} through the Ps^- photodetachment. A single peak is observed at $V_{\mathrm{acc}} = 1498$ V, however, as V_{acc} decreases, the peak splits into two peaks with respect to their respective mean TOF. This observation indicates an anisotropic photoelectron recoil effect with respect to the Ps^- traveling direction. When photoelectrons are emitted in the forward direction of travel of Ps^-, Ps is kicked rearward, resulting in a deceleration. Conversely, rearward emission leads to Ps being kicked forward, resulting in an acceleration. The separation of the Ps TOF peaks can be approximated by $L\sqrt{3m_{\mathrm{e}}E_{\mathrm{KER}}}/eV_{\mathrm{acc}}$, where m_e is the electron mass and e is the elementary charge, taking into account the back-to-back photoelectron emission. Once the separation exceeds the temporal width of the Ps atoms (2.2 ns FWHM), a double-peak structure clearly appears; V_{acc} must be less than 1500 V in the present setup. If V_{acc} is decreased, the separation between the two peaks on the TOF axis gradually increases as shown in Fig. 2. Moreover, it should be noted that the signal intensities decrease as V_{acc} is decreased due to the loss of short-lived Ps^- ions ($\tau = 479$ ps) [23] and o-Ps atoms ($\tau_{o\text{-Ps}} = 142$ ns) [24] by in-flight annihilation, and the energy dependence of the MCP detection efficiency.

To determine the distribution of photoelectron emission in the Ps^- photodetachment, TOF spectra were measured as a function of the polarization angle α, with V_{acc} fixed at 498 V, as shown in Fig. 3. The two peaks that are separated at $\alpha = 0$ become closer to each other as α is increased, resulting in a single peak at $\alpha = \pi/2$. With further increase in α, it again splits into two peaks and returns to a peak shape similar to that observed at $\alpha = 0$ and $\alpha = \pi$. Therefore, the photoelectron emission distribution is anisotropic with rotational symmetry.

For linearly polarized light, the photoelectron angular distribution (PAD) resulting from photoionization and photodetachment is formulated as [25,26]

$$\frac{d\sigma}{d\Omega} = \frac{\sigma_{\mathrm{t}}}{4\pi}\left\{1 + \frac{\beta}{2}(3\cos^2\vartheta - 1)\right\}, \tag{1}$$

where, σ_{t} and ϑ are the total cross section and the angle between the direction of the photoelectron and the polarization vector, $\vec{\varepsilon}$, respectively. β is the asymmetry parameter, which characterizes the PAD and ranges from $-1(d\sigma/d\Omega \propto \sin^2\vartheta)$ to $+2(d\sigma/d\Omega \propto \cos^2\vartheta)$. The projection of Eq. (1) onto the $x-y$ plane gives the probability distribution function of fragment Ps atoms as a function of the z-axis component of the recoil velocity, v_z, in the center of mass frame, represented by

$$f(v_{\mathrm{z}}) = \frac{\sigma_{\mathrm{t}}}{4}\left\{2 + \frac{\beta}{2}\left(3\sin^2\alpha + 3(2 - 3\sin^2\alpha)\left(\frac{v_{\mathrm{z}}}{v}\right)^2 - 2\right)\right\}. \tag{2}$$

Here, $v = \sqrt{E_{\mathrm{KER}}/3m_{\mathrm{e}}}$ is the speed of the fragment Ps in the center of mass frame. To transform the z-axis velocity form of Eq. (2) to a time form for the comparison with the TOF spectra obtained, we incorporate a time deviation, t', from the mean TOF, $\bar{t}$, due to the recoil velocity, v_z.

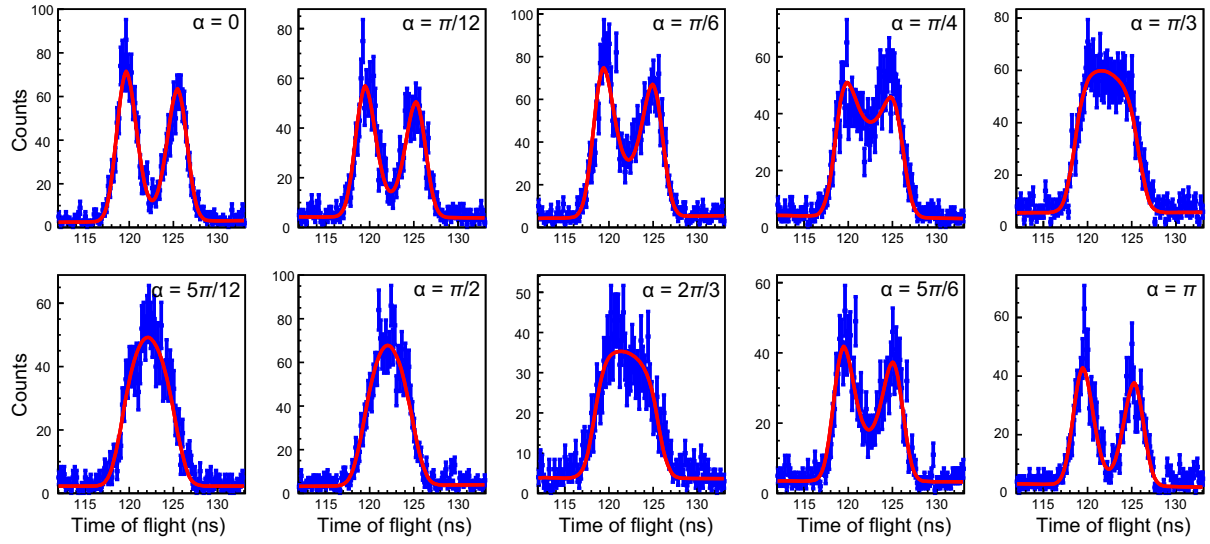

FIG. 3. Time-of-flight spectra of the fragment Ps atoms as a function of α, with V_{acc} fixed at 498 V. Each spectrum was accumulated over 7200 s. The red lines represent the least-squares fits with Eq. (3), by which all datasets were simultaneously fitted sharing the common parameter β.

Since $\bar{t}+t'=L/(V_z+v_z)$, where V_z is the z-axis component of the Ps^- ion velocity, v_z is approximated by $-V_z^2 t'/L$. Therefore Eq. (2) is transformed to the time form with v_z as

$$f(t') = Ce^{\frac{-t'}{\tau_{o\text{-Ps}}}}G(t')\left\{2+\frac{\beta}{2}\left(3\sin^2\alpha + 3(2-3\sin^2\alpha)\left(\frac{V_z^2 t'}{vL}\right)^2 - 2\right)\right\}, \qquad |t'| \le \frac{vL}{V_z^2};$$
$$f(t') = 0, \qquad |t'| > \frac{vL}{V_z^2}, \tag{3}$$

where C is a normalization factor. To reproduce the experimental data, two corrections have been made. The first pertains to the loss of the fragment o-Ps atoms due to in-flight annihilation, denoted by the exponential term. As the arrival times at the detector of the fragments that recoil forward and rearward differ, there is a slight difference in the in-flight losses. The second refers to the geometric loss term of those fragments that cannot pass through the pumping reducer, expressed as $G(t')$. The components with relatively high momentum in the radial direction ($x-y$ plane), specifically those o-Ps atoms with relatively small momentum in the travel direction (z axis) and lying near the mean TOF, become spatially lost due to the presence of the reducer and require correction. The Supplemental Material [27] describes the details of this systematic correction.

In the analysis of the TOF spectra, an evaluation of the response function arising from the detection system and the temporal profile of the illuminated Ps^- ions is required. By fitting the TOF spectrum at $V_{acc}=4998$ V and $\alpha=\pi/2$(σ polarization), where the recoil effect is negligible, with a single Gaussian distribution, the response function is evaluated to have a standard deviation of (0.93 ± 0.06) ns. Finally, the TOF spectra were fitted using the least-squares method with Eq. (3) convoluted with the response function and a linear background shown by the red line in Fig. 3. The electron affinity of o-Ps, E_B, in E_{KER} was fixed at the previously determined value of 0.3269 eV [13,28,29]. All datasets were fitted simultaneously with common parameters β and chi-square χ^2, resulting in $\beta=1.97\pm0.04$ [reduced chi-square $\chi^2/(N-m)=1149/1013$, where N and m are the number of data points and free parameters, respectively, the latter being 31]. The measured TOF spectra are well reproduced by the model function based on the PAD described above. Note that the intensities of the components kicked forward by the photoelectrons (the faster components on the TOF spectra) are significantly higher than those kicked rearward (the slower components). This phenomenon can be attributed to the aforementioned correction terms, namely in-flight annihilation and the geometric loss of fragment o-Ps atoms. Regarding the latter, the forward-kicked components have higher momentum in the travel direction than those kicked rearward, reducing the spatial spread and increasing the efficiency as they pass through the reducer tube.

Including the systematic uncertainty in the determination of the asymmetry parameter, β, as described in Appendix B, β was eventually determined to be $1.97\pm0.04(\text{stat})\pm0.07(\text{syst})$ in the one-photon detachment of Ps^- ions at a photon energy of 1.165 eV. A value of β close to 2 indicates that the PAD is anisotropic with respect to the polarization vector of the laser beam and follows a $\cos^2\vartheta$ distribution. The values of β, for the photodetachment of the l-orbital electron by linearly polarized light, are formulated according to the theory of Cooper and Zare [25]. This formulation is sensitive to the phase shift of the outgoing electron partial waves and the radial matrix elements of the dipole transition. Hanstorp [30] proposed a simplified formulation of β by replacing the nontrivial matrix elements with the reciprocal energy of the outgoing electron under the Wigner's assumption. These theories reproduce well the asymmetry parameter for the photoemission of various species [31,32]. In the present experiment, given the photon flux density, only one-photon detachment of the s-orbital electron ($l=0$) from Ps^- ($^1S^e$ state) occurs, resulting in a p-wave continuum electron and the residual Ps in the final state. Therefore, the formulation derives β to be 2, independent of the photon energy, which is consistent with the experimental value. This is the simplest case of the PAD in the photodetachment of an anion, analogous to the one-photon detachment of H^- ions [26]. To understand the photodissociation dynamics of Ps^- ions more in detail, in the future it might be worth investigating the PAD induced by two-photon detachment. In this scheme, interference between the s and d waves of the outgoing electron can significantly impact β, depending on the photon energy and laser field strength as observed in H^- [33,34]. The validity of existing theories can be tested against exotic particle systems. Furthermore, the PAD in the photodetachment via an autoionization (resonance) state may differ from the nonresonant PAD, as predicted by the Cooper and Zare theory [35]. While there is no theoretical research on the exotic Ps^- ion, measuring the PAD in the resonant scheme [12] could provide new dynamical information.

Translation recoil momentum spectroscopy, based on TOF measurements, is useful to investigate the angle-resolved photodissociation dynamics of exotic particle species composed of particles and their antiparticles, such as positrons [36,37] and muons [38], antiprotons [39]. Because of their rarity and short-lived nature, these species present significant challenges in the generation of cold and pointlike sources, which is far more difficult than for atoms and molecules. The photofragment imaging techniques [5–9] are not yet sufficient for various exotic particle systems, whereas the TOF-based method demonstrated in

this study proves to be applicable due to its simplicity and high collection efficiency of the fragments. As mentioned above, the dissociation kinetics of exotic species resembles that of molecular dissociations [19,20] because of the closed masses of the outgoing and residual fragments. This suggests that the fragments and residuals experience significant recoil, causing significant effects in the time domain to be observable.

In conclusion, we have demonstrated the recoil momentum spectroscopy of Ps^- ions using the TOF method and have observed the photoelectron-recoil kick to the Ps atom in the Ps^- photodetachment process. We examined the angular distribution of the photoelectrons by controlling the polarization vector of the linearly polarized IR laser beam used for the photodetachment. At the photon energy of 1.165 eV, the asymmetry parameter was found to be in agreement with the prediction by Cooper and Zare. The present technique could clarify the photodissociation dynamics of Ps^- ions by simply modifying the laser parameters, e.g., photon density, photon energy, and polarization (circular and elliptical). Moreover, in the dissociation of exotic particle species made of particles and their antiparticles having the same mass, the outgoing and residual fragments undergo a significant recoil similar to molecular dissociation. Measuring the recoil effects will create opportunities to explore the dissociation dynamics of exotic matter in a novel research field. On the other hand, we have shown that the anisotropic photoelectron emission in response to the laser polarization and their recoil have a significant effect on the momentum distribution of the fragment Ps atoms. This polarization effect enables us to manipulate various exotic particles, e.g., improve the quality of Ps beams and select the quantum states of Ps [14]. The expected coherent Ps beams would have great potential to explore surface structure analysis methods by diffraction [15] and test gravity effects on Ps [17,18].

We would like to thank A. Yagishita, Y. Nagata, and N. Oshima for meaningful discussions on this experiment. This work was supported by JSPS KAKENHI Grants No. JP21H04457, No. JP17H01074, and No. JP16K17705.

Appendix A: Background reduction on the detection system.—In the detection of the *o*-Ps atoms formed by the photodetachment of Ps^- ions, the charged particles, such as photoelectrons and secondary electrons, generated by positron impact onto the converter are eliminated by a pair of permanent magnets on the flight path (not shown in Fig. 1), so as to reduce serious background on the detection system [14]. Furthermore, although a fraction of the positrons are re-emitted from the Na-coated W surface, these are all eliminated by the electrostatic potential configuration that accelerates the negatively charged Ps^- ions. Thus, the electrically neutral *o*-Ps atoms and annihilation gamma rays from the converter are only detected by the MCP, allowing TOF measurements with high signal-to-background ratio. Since the kinetic energy of the Ps atoms of several hundred eV is relatively high, Ps can be detected by the MCP through the signal amplifications of direct secondary electron emission and fragment electrons generated by Ps dissociation on the MCP channel [40].

Appendix B: Systematic uncertainties.—The systematic uncertainty in the determination of β was evaluated as follows. The uncertainty in the standard deviation of the response function (± 0.06 ns) incorporated in the fitting affects the TOF spectral shape, resulting in a deviation from the maximum likelihood value of β to be 3.2%. The geometrical loss function, $G(t')$, was evaluated by a particle tracking simulation (see Supplemental Material [27]). Since the spatial distribution of the fragment Ps atoms depends on the PAD, this simulated function slightly depends on the conditions of the α and β values ranging between -1.0 and $+2.0$. Thus, the standard deviation of the determined values of β using $G(t')$ functions under various α and β conditions is assigned an uncertainty of 0.8%. Furthermore, the uncertainties of the drift length of Ps atoms, L, and the calibration of the polarization angle, α, contribute to 0.2% and 0.4%, respectively. Therefore, from the square root of these independent uncertainties, the systematic uncertainty was estimated to be 0.067 (3.4% of β value).

*Corresponding author: koji.michishio@aist.go.jp

[1] C. Y. Ng, *Photoionization, and Photodetachment (In 2 Parts)* (World Scientific, Inc., New York, 2000).
[2] D. J. Gendron and J. W. Hepburn, Dynamics of HI photodissociation in the A band absorption via H-atom Doppler spectroscopy, J. Chem. Phys. **109**, 7205 (1998).
[3] M. N. R. Ashfold, I. R. Lambert, D. H. Mordaunt, G. P. Morley, and C. M. Western, Photofragment translational spectroscopy, J. Phys. Chem. **96**, 2938 (1992).
[4] Z. Lu and R. E. Continetti, Dynamics of the acetyloxyl radical studied by dissociative photodetachment of the acetate anion, J. Phys. Chem. A **108**, 9962 (2004).
[5] H. J. Deyerl, L. S. Alconcel, and R. E. Continetti, Photodetachment imaging studies of the electron affinity of CF_3, J. Phys. Chem. A **105**, 552 (2001).
[6] E. Surber, R. Mabbs, and A. Sanov, Probing the electronic structure of small molecular anions by photoelectron imaging, J. Phys. Chem. A **107**, 8215 (2003).
[7] G. Aravind, N. Bhargava Ram, A. K. Gupta, and E. Krishnakumar, Probing the influence of channel coupling on the photoelectron angular distribution for the photodetachment from Cu^-, Phys. Rev. A **79**, 043411 (2009).
[8] R. Dörner, V. Mergel, O. Jagutzki, L. Spielberger, J. Ullrich, R. Moshammer, and H. Schmidt-Böcking, Cold target recoil ion momentum spectroscopy: A 'momentum microscope' to view atomic collision dynamics, Phys. Rep. **330**, 95 (2000).
[9] A. G. Suits, Invited review article: Photofragment imaging, Rev. Sci. Instrum. **89**, 111101 (2018).

[10] M. Emami-Razavi and J. W. Darewych, Review of experimental and theoretical research on positronium ions and molecules, Eur. Phys. J. D **75**, 188 (2021).

[11] Y. Nagashima, Experiments on positronium negative ions, Phys. Rep. **545**, 95 (2014).

[12] K. Michishio, T. Kanai, S. Kuma, T. Azuma, K. Wada, I. Mochizuki, T. Hyodo, A. Yagishita, and Y. Nagashima, Observation of a shape resonance of the positronium negative ion, Nat. Commun. **7**, 11060 (2016).

[13] K. Michishio, S. Kuma, Y. Nagata, L. Chiari, T. Iizuka, R. Mikami, T. Azuma, and Y. Nagashima, Threshold photodetachment spectroscopy of the positronium negative ion, Phys. Rev. Lett. **125**, 063001 (2020).

[14] K. Michishio, L. Chiari, F. Tanaka, N. Oshima, and Y. Nagashima, A high-quality and energy-tunable positronium beam system employing a trap-based positron beam, Rev. Sci. Instrum. **90**, 023305 (2019).

[15] K. F. Canter, *Low Energy Positron and Positronium Diffraction, Positron Scattering in Gases*, edited by J. W. Humberston and M. R. C. McDowell (Plenum, New York, 1983), pp. 219–225.

[16] S. J. Brawley, S. Armitage, J. Beale, D. E. Leslie, A. I. Williams, and G. Laricchia, Electron-like scattering of positronium, Science **330**, 789 (2010).

[17] A. P. Mills, Jr. and M. Leventhal, Can we measure the gravitational free fall of cold Rydberg state positronium?, Nucl. Instrum. Methods Phys. Res., Sect. B **192**, 102 (2002).

[18] G. Vinelli, F. Castelli, R. Ferragut, M. Romé, M. Sacerdoti, L. Salvi, V. Toso, M. Giammarchi, G. Rosi, and G. M. Tino, A large-momentum-transfer matter-wave interferometer to measure the effect of gravity on positronium, Classical Quantum Gravity **40**, 205024 (2023).

[19] S. R. Gandhi, T. J. Curtiss, and R. B. Bernstein, Asymmetry of the polarized-laser-induced photofragmentation of oriented CH_3I molecules, Phys. Rev. Lett. **59**, 2951 (1987).

[20] N. Saito and I. H. Suzuki, Asymmetry of departing fragment ion in the K-shell excitation of N_2, Phys. Rev. Lett. **61**, 2740 (1988).

[21] R. G. Greaves and J. Moxom, Design and performance of a trap-based positron beam source, AIP Conf. Proc. **692**, 140 (2003).

[22] H. Terabe, K. Michishio, T. Tachibana, and Y. Nagashima, Durable emission of positronium negative ions from Na-and K-coated W (100) surfaces, New J. Phys. **14**, 015003 (2012).

[23] H. Ceeh, C. Hugenschmidt, K. Schreckenbach, S. A. Gärtner, P. G. Thirolf, S. M. Fleischer, and D. Schwalm, Precision measurement of the decay rate of the negative positronium ion Ps^-, Phys. Rev. A **84**, 062508 (2011).

[24] Y. Kataoka, S. Asai, and T. Kobayashi. First test of $O(\alpha^2)$ correction of the orthopositronium decay rate, Phys. Lett. B **671**, 219 (2009).

[25] J. Cooper and R. N. Zare, Angular distribution of photoelectrons, J. Chem. Phys. **48**, 942 (1968).

[26] J. L. Hall and M. W. Siegel, Angular dependence of the laser photodetachment of the negative ions of carbon, oxygen, and hydrogen, J. Chem. Phys. **48**, 943 (1968).

[27] See Supplemental Material at http://link.aps.org/supplemental/10.1103/PhysRevLett.132.203001 for details on the geometrical loss function.

[28] A. M. Frolov, Bound-state properties of the positronium negative ion Ps^-, Phys. Rev. A **60**, 2834 (1999).

[29] G. W. F. Drake and M. Grigorescu, Binding energy of the positronium negative ion: Relativistic and QED energy shifts, J. Phys. B **38**, 3377 (2005).

[30] D. Hanstorp, C. Bengtsson, and D. J. Larson, Angular distributions in photodetachment from O^-, Phys. Rev. A **40**, 670 (1989).

[31] A. M. Covington *et al.*, Measurements of partial cross sections and photoelectron angular distributions for the photodetachment of Fe^- and Cu^- at visible photon wavelengths, Phys. Rev. A **75**, 022711 (2007).

[32] O. Windelius, J. Welander, A. Aleman, D. J. Pegg, K. V. Jayaprasad, S. Ali, and D. Hanstorp, Photoelectron angular distributions in photodetachment from P^-, Phys. Rev. A **103**, 033108 (2021).

[33] R. Reichle, H. Helm, and I. Y. Kiyan, Photodetachment of H^- in a strong infrared laser field, Phys. Rev. Lett. **87**, 243001 (2001).

[34] R. Reichle, H. Hanspeter, and I. Y. Kiyan, Detailed comparison of theory and experiment of strong-field photodetachment of the negative hydrogen ion, Phys. Rev. A **68**, 063404 (2003).

[35] D. Dill, Resonances in photoelectron angular distributions, Phys. Rev. A **7**, 1976 (1973).

[36] T. E. Wall, A. M. Alonso, B. S. Cooper, A. Deller, S. D. Hogan, and D. B. Cassidy, Selective production of Rydberg-Stark states of positronium, Phys. Rev. Lett. **114**, 173001 (2015).

[37] D. B. Cassidy and A. P. Mills, Jr., The production of molecular positronium, Nature (London) **449**, 195 (2007).

[38] S. J. Brodsky and R. F. Lebed, Production of the smallest QED atom: True muonium ($\mu^+\mu^-$), Phys. Rev. Lett. **102**, 213401 (2009).

[39] M. Doser, Antiprotonic bound systems, Prog. Part. Nucl. Phys. **125**, 103964 (2022).

[40] D. W. Gidley, R. Mayer, W. E. Frieze, and K. G. Lynn, Glancing angle scattering and neutralization of a positron beam at metal surfaces, Phys. Rev. Lett. **58**, 595 (1987).